Available online at www.sciencedirect.com
ScienceDirect
Biochemical and Biophysical Research Communications 369 (2008) 213–219
BBRC
www.elsevier.com/locate/ybbrc

Predominant role of type 1 IP_3 receptor in aortic vascular muscle contraction

Hong Zhou [a,f], Takeshi Nakamura [c,d,1], Nagisa Matsumoto [b,1], Chihiro Hisatsune [a,1], Akihiro Mizutani [b], Takafumi Iesaki [e], Hiroyuki Daida [e], Katsuhiko Mikoshiba [a,b,c,*]

[a] *Laboratory for Developmental Neurobiology, Brain Science Institute, RIKEN, 2-1 Hirosawa, Wako, Saitama 351-0198, Japan*
[b] *Division of Molecular Neurobiology, The Institute of Medical Science, The University of Tokyo, 4-6-1 Shirokanedai, Minato-ku, Tokyo 108-8639, Japan*
[c] *Calcium Oscillation Project, ICORP, Japan Science and Technology Corporation (JST), 3-14-4 Shirokanedai, Minato-ku, Tokyo 108-0071, Japan*
[d] *Department of Physiology, Juntendo University School of Medicine, 2-1-1, Hongo, Bunkyo-ku, Tokyo 113-8421, Japan*
[e] *Department of Cardiology, Juntendo University School of Medicine, 2-1-1, Hongo, Bunkyo-ku, Tokyo 113-8421, Japan*
[f] *Department of Pharmacology, School of Basic Medical Sciences, Peking University, Beijing 100083, China*

Received 15 October 2007
Available online 30 January 2008

Abstract

Inositol 1,4,5-trisphosphate receptor (IP_3R) plays a crucial role in generating Ca^{2+} signaling and three subtypes of IP_3R have been identified. In spite of a high degree of similarity among these subtypes, their effects on spatio-temporal Ca^{2+} patterns are specific and diverse; therefore the physiological significance of the differential expression levels of IP_3R subtypes in various tissues remains unknown. Here, we examined the relative contribution of the specific subtype of IP_3Rs to the agonist-induced Ca^{2+} signaling and contraction in IP_3R-deficient vascular smooth muscle cells and found that IP_3R1 deficient cells exclusively showed less sensitivity to the agonist, compared to those from the other genotypes. We also found that IP_3R1 dominantly expressed in vascular aortae on a consistent basis, and that phenylephrine (PE)-induced aortic muscle contraction was reduced specifically in IP_3R1-deficient aortae. Taken together, we concluded that IP_3R1 plays a predominant role in the function of the vascular smooth muscle *in vivo*.

Keywords: Thoracic aorta vascular smooth muscle cells; 2-Aminoethyl diphenylborinate; Phenylephrine

Inositol 1,4,5-trisphosphate receptor (IP_3R) is an important channel that controls Ca^{2+} signaling with varieties of spatio-temporal patterns [1]. To date, three mammalian IP_3R isoforms have been identified, which share 60–70% amino acid homology [2] and almost all tissues and cell lines express the three IP_3R subtypes to varying degrees [3]. However, the difference in their functional significance *in vivo* has been only partially understood. Gene targeting is one of the powerful tools used to reveal the functional role of a specific IP_3R subtype in tissues of interest. IP_3R1 is highly expressed in the central nervous system, particularly in the cerebellum [4] and the targeted deletion of IP_3R1 gene in mice caused ataxia and epileptic seizures, followed by a premature death, highlighting the importance of IP_3R1 for brain function [5]. IP_3R2 and IP_3R3 are involved in exocrine secretion, as inferred by a double deficiency of IP_3R2 and IP_3R3 showing deficit of saliva and pancreatic juice secretion [6].

An important step in the vascular smooth muscle contractile process is an increase in the intracellular Ca^{2+} concentration. It is now well established that the major pathway for increasing intracellular Ca^{2+} in smooth muscle is the activation of phospholipase C (PLC) via activation of a plasma membrane receptor, which leads to the production of IP_3. IP_3 then binds to IP_3Rs on the sarcoplasmic reticulum (SR) membrane and triggers the release of Ca^{2+}, thereby inducing contraction [7]. Thus, IP_3-induced

* Corresponding author. Fax: +81 48 467 9746.
E-mail address: mikosiba@brain.riken.go.jp (K. Mikoshiba).
[1] Equally contributed to this work.

0006-291X/$ - see front matter © 2008 Elsevier Inc. All rights reserved.
doi:10.1016/j.bbrc.2007.12.194

calcium release is an important triggering step for excitation-contraction coupling in the smooth muscles.

In vascular smooth muscle cells, expression of IP_3R subtypes is controversial; some reported IP_3R1 and IP_3R3 expression [3,8,9], whereas others reported the expression of IP_3R1 and IP_3R2 [10] in vascular muscle. In A7r5, a cell line derived from embryonic rat aorta, IP_3R1 and IP_3R3 are expressed with the type 1 isoform being predominant (~80% of IP_3Rs) [11]. In addition, IP_3R1 is shown to be more important than IP_3R3 for IP_3-induced Ca^{2+} release (IICR), capacitative calcium entry (CCE), and proliferation in A7r5 cells [11]. However, there has been no direct evidence showing the functional roles of specific IP_3R subtype in the intact vascular smooth muscle, such as primary cultured cells or *in situ* isolated muscle preparation. In this study, we investigated the agonist-induced Ca^{2+} responses and aortic muscle contraction in specific IP_3R-deficient mice and determined the relative contribution of specific IP_3R subtype to IICR and stimulus-contraction in the aortic vascular smooth muscle.

Materials and methods

Animals. IP_3R1 knockout (KO), IP_3R2KO, IP_3R3KO, $IP_3R2/3KO$ were described as previously [5,6].

The primary culture of mouse thoracic aorta vascular smooth muscle cells (TASMCs). Mouse TASMCs were isolated from thoracic aorta as previously described [12,13]. Mice (P15) were anesthetized with ethyl ether, killed by cervical dislocation, and thoracic aorta was quickly removed from all mice. Blood vessels were carefully cleaned of connective tissue, the tunica adventitia, and removed the endothelium by gently rubbing with a sterile cotton swab. Then, the remaining part of the aorta was cut into small pieces. The pieces of aorta were incubated in HBSS supplemented with 2 mg/ml collagenase, 0.5 mg/ml elastase, and 0.5 mg/ml trypsin inhibitor for 25 min at 37 °C. Enzymatic digestion was terminated by the addition of 5.0 ml CS-C Medium. The cell suspension was centrifuged, and the pellet was resuspended in CS-C medium containing 10% fetal bovine serum, 100 U/ml of penicillin G, and 10 mg/ml of streptomycin. The cell suspension was grown on 35-mm glass-bottom dishes at 37 °C in a humidified atmosphere of 5% CO_2 for 5–7 days until the cells became subconfluent.

Immunoblot analysis. Tissue samples of thoracic aorta were prepared as described above. The smooth muscle layer was teased away from the outer connective tissue layer and cut into pieces. Then, the pieces of tissue were homogenized for 90 s in homogenization medium [0.32 M sucrose, 1.0 mM EDTA, 5 mM Tris–HCl (pH 7.5)]. The homogenate was centrifuged for 5 min at 5000 rpm. The protein concentration of supernatants was determined and the proteins were separated by a 4.5–10% gradient SDS–PAGE and transferred to PVDF membrane. Primary antibodies used were 4C11 for IP_3R-1, ABsII for IP_3R-2 (king gift from Dr. A. Tanimura), anti-IP_3R3 antibody (Transduction Laboratories, BD Biosciencesfor), and anti-β-actin antibody. The membrane was incubated with horseradish peroxidase (HRP)-conjugated anti-mouse IgG (Amersham) for IP_3R1, IP_3R3, β-actin and HRP-conjugated anti-rabbit IgG for IP_3R2 as the secondary antibody. After washing with PBS-T, the immunoreactive bands were visualized by ECL-plus (for IP_3Rs) and ECL (for β-actin) detection system (Amersham Pharmacia Biotech).

The expression of IP_3 sponge in TASMCs. The expression vector for GFP-tagged IP_3 sponge was described previously [14]. For the transfection experiments, primarily cultured TASMCs were grown on 35-mm glass-bottom micro-well dishes and transfected by using TransIT transfection reagents (Mirus) according to the manufacturer's instructions. Five days after transfection, the cells were used for Ca^{2+} imaging.

Ca^{2+} imaging. Twenty-four hours before each experiment, the culture medium containing 10% FBS was substituted for the serum-free medium to arrest cell growth, allowing for establishment of steady state cellular events independent of cell division to prevent a false estimate of intracellular Ca^{2+} concentration. TASMCs were washed twice with BSS [(in mM) NaCl 125, KCl 5, $MgSO_4$ 1.2, glucose 11, $CaCl_2$ 1.8, and HEPES 25, at pH 7.4 adjusted with NaOH]. TASMCs were then loaded with 3 μM fura2-AM and 0.1% bovine serum albumin (BSA) in BSS for 45 min at room temperature. Then, the fura-2-loaded cells were then placed on the stage of an inverted fluorescence microscope (IX-70; Olympus, Japan) and perfused continuously at a rate of 1.0 ml/min with BSS. Image capturing and processing were done using a PC-driven software (Argus 50/CA; Hamamatsu Photonics, Japan). With alternate illumination at 340 and 380 nm excitation, pairs of the fluorescence images through an emission filter (510–550 nm) were obtained every 10 s using a silicon-intensified-target video camera (C2400-8; Hamamatsu Photonics, Japan), and digitized by an image processor (Argus50; Hamamatsu Photonics, Japan). For Ca^{2+}-free solution, $CaCl_2$ was omitted from BSS, and 2 mM EGTA was added.

Force measurement in isolated mouse aorta. Aortic vessel preparations were prepared from 16–20-day-old mice lacking specific subtype of IP_3R and age-matched WT littermates. Following sacrifice by heart puncture under deep anesthesia with diethylether, thoracic aortas were immediately dissected, rinsed in ice-cold PBS, and then connective tissue and fat were removed. Thoracic aorta rings in 2 mm length were taken, mounted in a chamber bath containing 5 ml Krebs–Henseleit solution [(in mM) NaCl 119, KCl 4.6, $NaHCO_3$ 15, $CaCl_2$ 1.5, $MgCl_2$ 1.2, NaH_2PO_4 1.2, glucose 5.5, pH 7.4], and connected to a Harvard apparatus differential capacitor force transducer (UFER magnus system, UFER medical instrument). The physiological salt solution was bubbled continuously with a mixture of 95% O_2 and 5.0% CO_2 at 37 °C. The segments were equilibrated at 125 mgf resting tension for 30 min. For recording a cumulative response-curve, increasing concentrations of PE in the range of 10^{-8} to 10^{-6} M were added, respectively, following the recording of high (30 mM) K^+-stimulated contraction, after each response reached a steady state. The extent of PE-induced contraction was expressed as a percentage of high K^+-stimulated contraction.

Results

Agonist-induced Ca^{2+} increases in cultured TASMCs

We cultured WT TASMCs and examined the nature of the ATP-induced $[Ca^{2+}]_i$ increases in them. About 90% of the cultured cells were α-actin positive, confirming the cells to be smooth muscle cells (Fig. 1A). Application of ATP to the cultured TASMCs induced Ca^{2+} signals, which was inhibited by 100 μM of 2-Aminoethyl diphenylborinate (2-APB) that is known to inhibit IICR (Fig. 1B). ATP-induced Ca^{2+} signals were also inhibited by the expression of IP_3-sponge, an IP_3-absorbent, into the cells (Fig. 1C) and by the PLC inhibitor, U-73122 (Fig. 1D), but not by U73343, a negative control for U73122 (data not shown). Based on these results, we concluded that the ATP-induced $[Ca^{2+}]_i$ increases in the cultured TASMCs were mediated by IP_3-induced Ca^{2+} release. We also tried to assess the responsiveness of the cultured TASMCs to several other agonists—PE, endothelin-1, and vasopressin—but only ATP reproducibly induced robust $[Ca^{2+}]_i$ increases in a dose-dependent manner in WT-cultured TASMCs. This is presumably due to somewhat phenotypic conversion to the de-differentiated properties, which is observed in the cultured smooth muscle cells in the proliferative phase [15,16], and thus we decided to use ATP as an agonist to

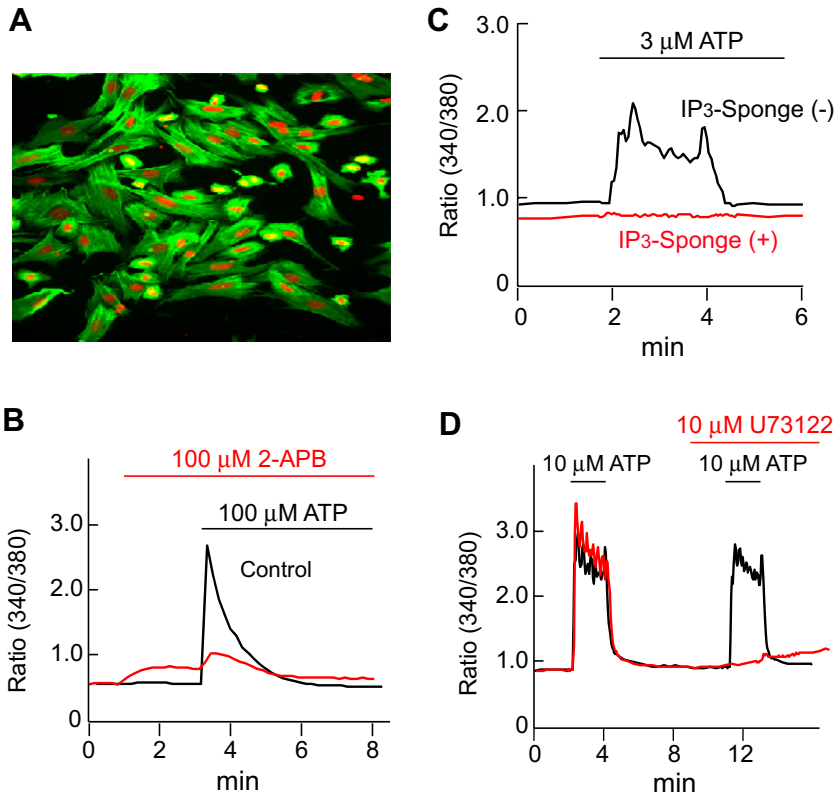

Fig. 1. Agonist-induced Ca^{2+} increases in cultured WT TASMCs. (A) Immunostaining of cultured WT TASMCs with anti-α-actin antibody (Green) and PI (Red). (B) The effect of 2-APB on ATP-induced $[Ca^{2+}]_i$ responses. ATP-induced $[Ca^{2+}]_i$ responses were recorded in the presence of 0.1% DMSO (black) or 100 μM 2-APB (red), in the Ca^{2+}-free buffer containing 2 mM EGTA. (C) Effect of the expression of IP_3-sponge on ATP-induced $[Ca^{2+}]_i$ responses. The red and black traces represent Ca^{2+} signals in TASMCs with and without IP_3-sponge, respectively. (D) Effect of U73122 on ATP-induced Ca^{2+} release in the presence of extracellular Ca^{2+}.

quantitatively analyze the Ca^{2+} signals in vascular smooth muscle cells in the following study.

IP_3R1 plays important role in ATP-induced Ca^{2+} signals in TASMCs

Next, we used IP_3RKO TASMCs to determine the IP_3R subtype responsible for Ca^{2+} signals in the vascular smooth muscle. There were no significant morphological difference between cultured WT and IP_3RKO TASMCs. Immunostaining of cultured cells with anti-smooth muscle α-actin antibody and propidium iodide revealed that about 92.95%, 93.84%, 94.74%, 94.89%, and 96.03% of the cells were α-actin positive in cultured IP_3R1KO, IP_3R2KO, IP_3R3KO, and IP_3R2/3KO cells, respectively, indicating that the lack of IP_3Rs did not profoundly affect on the smooth muscle differentiation (Supplemental Fig. 1).

We stimulated cultured WT TASMCs with various concentrations of ATP (1.0, 3.0, 10, and 100 μM) and examined the intracellular Ca^{2+} signals in the absence of extracellular Ca^{2+} (Ca^{2+}-free BSS with 2 mM EGTA). WT TASMCs dose-dependently responded to ATP from 1.0 to 100 μM. Cultured IP_3R2KO, IP_3R3KO, and IP_3R2/3 double KO TASMCs also showed Ca^{2+} signals in response to 1.0, 3.0, 10, and 100 μM ATP similar to those in the WT cells, whereas IP_3R1KO TASMCs failed to respond to 1.0 μM ATP as shown in Fig. 2. In addition, the peak amplitude in response to 3.0 and 10 μM ATP was significantly decreased in IP_3R1KO TASMCs compared to WT cells. Thus, these results demonstrated that IP_3R1 plays a predominant role in Ca^{2+} signaling in response to ATP.

IP_3R1 was predominantly expressed in aorta

We next examined the expression level of each IP_3R subtype in aorta using the subtype-specific anti-IP_3R antibodies and pan-IP_3R antibody that recognizes all IP_3R subtypes in a similar level [17]. We used P15 WT and IP_3RKO mice, because IP_3R1KO mice die within 21 days. In aortae from P15 WT mice, we detected the expression of all subtypes of IP_3Rs with subtype-specific anti-IP_3R antibodies (Fig. 3A). Anti-Pan-IP_3R antibodies detected two bands corresponding to IP_3R1 (upper band) and IP_3R2 or IP_3R3 (lower bands) (Fig. 3A). The upper band was stronger than the lower one in WT aortae, indicating that IP_3R1 was predominantly expressed in aortae. The lower band was detected in IP_3R2KO aorta in a similar level to WT, but disappeared in IP_3R3KO aortae. Thus, these results indicated that aorta expressed each subtypes of

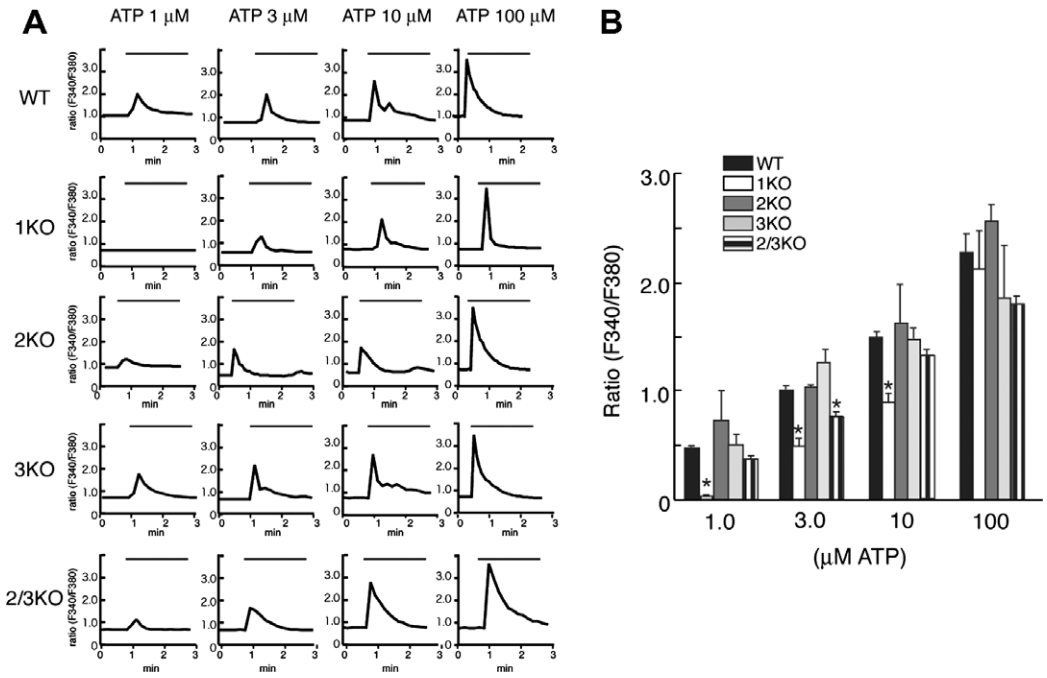

Fig. 2. ATP-induced Ca^{2+} signals in WT and IP_3R-deficient TASMCs. (A) Traces are the average responses to various concentration of ATP in at least 50 individual cells from a single experiment and are representative of more than three independent experiments. (B) Mean peak amplitude of Ca^{2+} signals in response to various concentration of ATP.

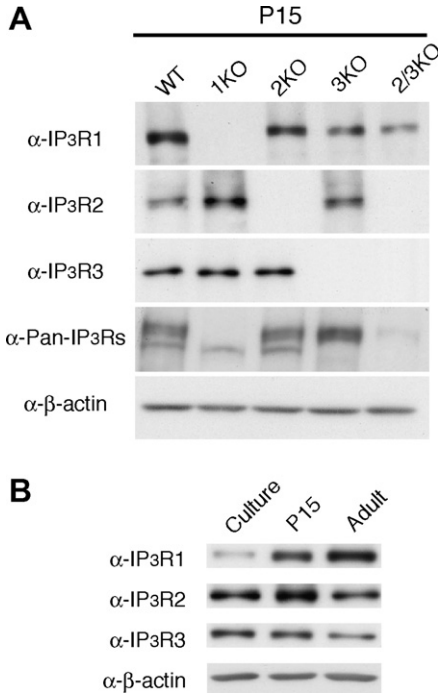

Fig. 3. The expression level of each IP_3R subtype in aortic vascular tissue. The expression level of each IP_3Rs in P15 (A) or adult and cultured (B) thoracic aorta vascular smooth muscle from WT and various IP_3RKO mouse. The experiments were performed three times and the representative data are shown.

IP_3Rs in the order of $IP_3R1 > IP_3R3 >> IP_3R2$ in P15, and the expression level of IP_3R2 is very small among the three subtypes of IP_3Rs. We also examined the IP_3R expression in adult aortae and the cultured TASMCs. As shown in Fig. 3B, all subtypes of IP_3Rs were again detected in both adult aortae and cultured TASMCs but in different ratio compared to P15 mice. Expression of IP_3R1 was increased and that of IP_3R3 was decreased as mice became older from P15 to adult (Fig. 3B). In cultured TASMCs, we detected a lesser amount of IP_3R1 expression and a greater amount of IP_3R3 expression as compared to P15 WT aortae (Fig. 3B).

Reduced phenylephrine-induced aorta contraction in IP_3R1KO mice

Finally, we examined the role of specific IP_3R subtypes in the stimulus-induced contraction of the vascular smooth muscle *in vivo* using the aortae. There were no significant histological differences in thoracic aorta tissue structures between WT and IP_3RKO mice, suggesting that IP_3R deficiency in any subtype did not significantly affect the development of the arterial vascular smooth muscles *in vivo* (Supplemental Fig. 2). Nevertheless, there was a possibility that further analysis will reveal a subtle difference. We first stimulated aortic rings of IP_3RKO and WT mice with high K^+ (30 mM) and after the high K^+-induced contraction was returned to the baseline level, cumulative concentrations (10^{-8} to 10^{-6} M) of PE were applied (Fig. 4A). Because force generation actually varies among the aortae used, we used these two stimuli to evaluate the contractility of the aorta and presented the PE-induced contraction to the percentage of the high K^+-induced contraction that exhibits maximal contraction. The normalization allowed

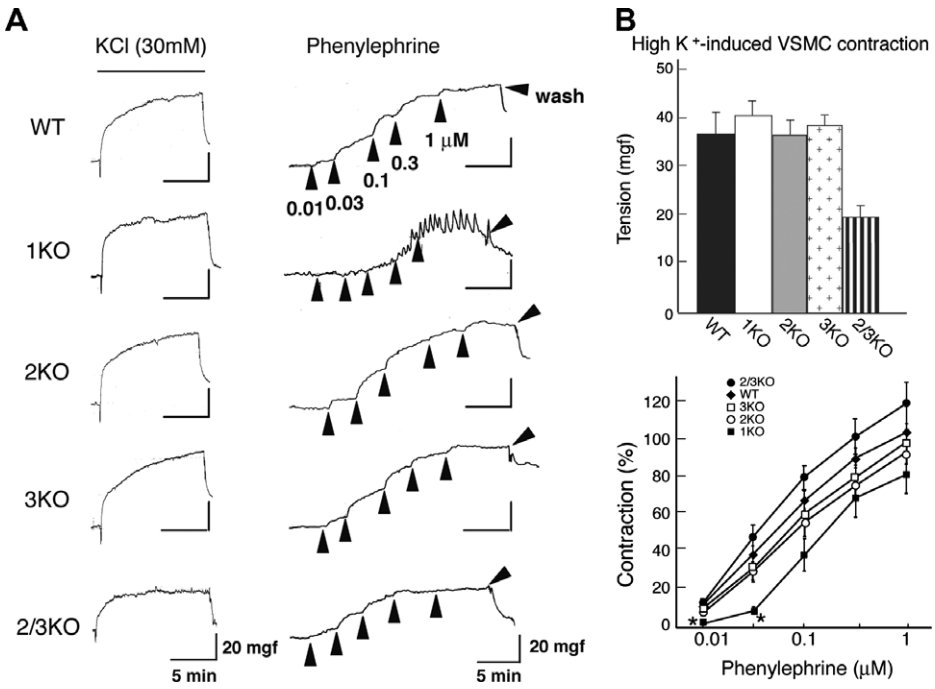

Fig. 4. Decreased PE-induced isometric force in IP_3R1KO aorta. (A) KCl-dependent contraction (left) and PE-dependent contraction (right) in aortic rings isolated from aorta of WT and various IP_3R KO mice. (B) Comparison of the isomeric force evoked by KCl and PE in WT and mutant aortas. *Upper panel:* high KCl-induced vascular smooth muscle cell contraction. *Lower panel:* dose-dependent PE-induced contraction. Data are expressed as a percentage of 30 mM KCl-induced contraction. Data represents the mean ± SEM (WT, $n = 8$; IP_31KO, $n = 7$; IP_32KO, $n = 6$; IP_33KO, $n = 7$; $IP_32/3KO$, $n = 6$). *Statistically significant ($p < 0.05$, *t*-test).

us to quantitatively compare the difference in PE-induced contractility between each genotype of mice. As shown in Fig. 4A, we found that the aorta isolated from IP_3R1KO mice failed to respond to low concentrations of PE up to 1.0 μM, whereas those from other genotypes responded dose-dependently (Fig. 4B, upper panel). The KCl-induced aortic contraction in IP_3R1 deficient aorta was observed to be similar to the level in WT (Fig. 4A). The reason for the decreased contractility of $IP_3R2/3$ double KO aortae in response to high K^+ stimulation was unknown, but may be related to the malnutrition seen in $IP_3R2/3$ double KO mice [6]. Nevertheless, the $IP_3R2/3$ double KO aorta contracted in response to low concentrations of PE as similar to that seen in WT aortae (Fig. 4B, lower panel), supporting the predominant role of IP_3R1 in PE-induced contractility. Thus, although the machinery contributing to muscle contraction, such as the acto-myosin system, seemed to be fully functional, agonist-induced contraction was impaired in IP_3R1KO aorta, indicating the predominant role of the IP_3R1 in the stimulus-contraction coupling mechanism in vascular smooth muscles.

Discussion

In this study, we examined the functional role of a specific IP_3R subtype in vascular smooth muscle by examining the difference in ATP-induced Ca^{2+} responses between WT and IP_3RKO. We found that the 1.0 μM of ATP-induced an intracellular Ca^{2+} increase in IP_3R2KO and IP_3R3KO TASMCs similar to that seen in WT cells, but not in IP_3R1KO cells. Moreover, peak amplitude of Ca^{2+} signals in response to 3 and 10 μM ATP stimulation was apparently decreased in IP_3R1KO TASMCs. Notably, the TASMCs cultured from $IP_3R2/3$ double KO mice were able to induce Ca^{2+} signals in response to stimulation with 1.0 μM ATP. Consistent with this, we demonstrated the reduced stimulus-contraction in IP_3R1KO aorta. Since the expression levels of IP_3R2 and 3 subtypes were not significantly changed (Fig. 3), the lower sensitivity of IP_3R1 KO aorta to PE was not due to the changes in the expression levels of the other IP_3R subtypes. These results indicate a preferential role of IP_3R1 in the induction of $[Ca^{2+}]_i$ signaling in the vascular smooth muscle cells.

The expression of IP_3R subtypes in mouse aortae (Fig. 3) in our study was virtually similar to the previous data on rat aortae [3,8,9]. The IP_3R subtype expression changed during postnatal development, with IP_3R3 being predominant in neonate and young vascular smooth muscle and IP_3R1 being increased during development. In our culture condition, the level of IP_3R1 expression was lower than that in P15 and adult, but nevertheless IP_3R1 expression was highest among the three types of IP_3Rs (Fig. 3). Because the preferential role of IP_3R1 in Ca^{2+} signaling was still observed even under the culture condition where IP_3R1 was down-regulated, the role of IP_3R1 in adult aortae when IP_3R1 expression increases would be inevitable. It has been known that IP_3R1 has a higher IP_3 binding affinity than

IP_3R3 and that the threshold of Ca^{2+} concentration facilitating IP_3R activity is lower for IP_3R1 than for IP_3R3 [18]. Presumably, because of these properties, the IP_3R1 subtype has a lower threshold for agonist concentration in inducing IICR.

While the IP_3R1KO aorta showed high K^+-induced contraction indistinguishable from IP_3R2KO and IP_3R3KO aortae, it failed to respond to low concentrations of PE. The data indicated that although the machinery contributing to muscle contraction, such as the actin-myosin system, was intact in IP_3R1KO aorta, contraction induced by low concentration of agonists was impaired. This indicates the predominant involvement of IP_3R1 subtype in the stimulation–contraction coupling mechanism in vascular smooth muscles. This idea is further strengthened by the data that the aortae isolated from $IP_3R2/3$-double KO mice normally contracted in response to low concentrations of PE, although it showed decreased K^+-induced contraction. Since the IP_3R1 expression level in the adult aorta was higher than that in P15 (Fig. 3B), the IP_3R1 may potentially play a more predominant role in adult aorta function than in P15 mice tested in the present study.

Using the A7r5 cells, Wang et al. showed the critical role of IP_3R1 in the proliferation of vascular smooth muscle cells [11]. On the other hand, Tasker et al. described that IP_3R3 has an important role as a predominant subtype during the developing period in the vascular smooth muscle cell growth [9]. However, we did not observe the significant retardation of cell growth in the IP_3R1KO cells, besides, IP_3R2, IP_3R3, or $IP_3R2/3$ double KO cells (data not shown). Consistently, the aortae were normally formed in any genotypes of the IP_3R-deficient mice, suggesting a redundant role of IP_3R subtypes in the growth of vascular smooth muscle cells (Supplemental Fig. 2). Most likely, any subtypes of IP_3R can redundantly work for cell growth, as long as a sufficient amount of the receptors necessary for proliferation are functionally expressed. Otherwise, the increased expression of IP_3R3 in the primary cultured vascular smooth muscle cell (Fig. 3) would lead to no retardation of cell growth in the IP_3R1KO cells, unlike A7r5 cells.

It is known that IP_3R1-deficient mice die within 21 days after birth [5,6]. The lack of the functional role of IP_3R1 in smooth muscle may be one of the reasons for the early death of IP_3R1KO mice. Further analysis using tissue specific IP_3R1-deficient mice will elucidate the relationship between the role of IP_3R1 in various tissues and the phenotype of IP_3R1KO mice.

Acknowledgments

We thank Dr. A. Tanimura for anti-IP_3R2 antibody (ABsII) and all members of our laboratories for experimental helps and advices. Supported by grants from the Ministry of Education, Science, and Culture of Japan (K.M. and A.M.) and Grant-in-Aid for Young Scientists (C.H.), and the Japan Science and Technology Agency.

Appendix A. Supplementary data

Supplementary data associated with this article can be found, in the online version, at doi:10.1016/j.bbrc.2007.12.194.

References

[1] M.J. Berridge, P. Lipp, M.D. Bootman, The versatility and universality of calcium signalling, Nat. Rev. Mol. Cell Biol. 1 (2000) 11–21.
[2] T. Furuichi, K. Mikoshiba, Inositol 1, 4, 5-trisphosphate receptor-mediated Ca2+ signaling in the brain, J. Neurochem. 64 (1995) 953–960.
[3] H. De Smedt, L. Missiaen, J.B. Parys, M.D. Bootman, L. Mertens, L. Van Den Bosch, R. Casteels, Determination of relative amounts of inositol trisphosphate receptor mRNA isoforms by ratio polymerase chain reaction, J. Biol. Chem. 269 (1994) 21691–21698.
[4] T. Furuichi, S. Yoshikawa, A. Miyawaki, K. Wada, N. Maeda, K. Mikoshiba, Primary structure and functional expression of the inositol 1,4,5-trisphosphate-binding protein P400, Nature 342 (1989) 32–38.
[5] M. Matsumoto, T. Nakagawa, T. Inoue, E. Nagata, K. Tanaka, H. Takano, O. Minowa, J. Kuno, S. Sakakibara, M. Yamada, H. Yoneshima, A. Miyawaki, Y. Fukuuchi, T. Furuichi, H. Okano, K. Mikoshiba, T. Noda, Ataxia and epileptic seizures in mice lacking type 1 inositol 1,4,5-trisphosphate receptor, Nature 379 (1996) 168–171.
[6] A. Futatsugi, T. Nakamura, M.K. Yamada, E. Ebisui, K. Nakamura, K. Uchida, T. Kitaguchi, H. Takahashi-Iwanaga, T. Noda, J. Aruga, K. Mikoshiba, IP_3 receptor types 2 and 3 mediate exocrine secretion underlying energy metabolism, Science 309 (2005) 2232–2234.
[7] S. Kobayashi, T. Kitazawa, A.V. Somlyo, A.P. Somlyo, Cytosolic heparin inhibits muscarinic and alpha-adrenergic Ca2+ release in smooth muscle. Physiological role of inositol 1,4,5-trisphosphate in pharmacomechanical coupling, J. Biol. Chem. 264 (1989) 17997–18004.
[8] M.O. Islam, Y. Yoshida, T. Koga, M. Kojima, K. Kangawa, S. Imai, Isolation and characterization of vascular smooth muscle inositol 1,4,5-trisphosphate receptor, Biochem. J. 316 (Pt 1) (1996) 295–302.
[9] P.N. Tasker, F. Michelangeli, G.F. Nixon, Expression and distribution of the type 1 and type 3 inositol 1,4, 5-trisphosphate receptor in developing vascular smooth muscle, Circ. Res. 84 (1999) 536–542.
[10] O. Vallot, L. Combettes, P. Jourdon, J. Inamo, I. Marty, M. Claret, A.M. Lompre, Intracellular Ca^{2+} handling in vascular smooth muscle cells is affected by proliferation, Arterioscler. Thromb. Vasc. Biol. 20 (2000) 1225–1235.
[11] Y. Wang, J. Chen, Y. Wang, C.W. Taylor, Y. Hirata, H. Hagiwara, K. Mikoshiba, T. Toyo-oka, M. Omata, Y. Sakaki, Crucial role of type 1, but not type 3, inositol 1,4,5-trisphosphate (IP3) receptors in IP3-induced Ca2+ release, capacitative Ca2+ entry, and proliferation of A7r5 vascular smooth muscle cells, Circ. Res. 88 (2001) 202–209.
[12] Y. Hirakawa, M. Gericke, R.A. Cohen, V.M. Bolotina, Ca^{2+}-dependent Cl(−) channels in mouse and rabbit aortic smooth muscle cells: regulation by intracellular Ca^{2+} and NO, Am. J. Physiol. 277 (1999) H1732–H1744.
[13] H. Hamada, D.S. Damron, S.J. Hong, D.R. Van Wagoner, P.A. Murray, Phenylephrine-induced Ca^{2+} oscillations in canine pulmonary artery smooth muscle cells, Circ. Res. 81 (1997) 812–823.
[14] T. Uchiyama, F. Yoshikawa, A. Hishida, T. Furuichi, K. Mikoshiba, A novel recombinant hyperaffinity inositol 1,4,5-trisphosphate (IP_3) absorbent traps IP_3, resulting in specific inhibition of IP(3)-mediated calcium signaling, J. Biol. Chem. 277 (2002) 8106–8113.
[15] W.S. Shin, T. Toyo-oka, M. Masuo, Y. Okai, H. Fujita, T. Sugimoto, Subpopulations of rat vascular smooth muscle cells as discriminated by calcium release mechanisms from internal stores, Circ. Res. 69 (1991) 551–556.
[16] M. Masuo, T. Toyo-oka, W.S. Shin, T. Sugimoto, Growth-dependent alterations of intracellular Ca^{2+}-handling mechanisms of vascular

smooth muscle cells. PDGF negatively regulates functional expression of voltage-dependent, IP3-mediated, and Ca^{2+}-induced Ca^{2+} release channels, Circ. Res. 69 (1991) 1327–1339.

[17] M. Hattori, A.Z. Suzuki, T. Higo, H. Miyauchi, T. Michikawa, T. Nakamura, T. Inoue, K. Mikoshiba, Distinct roles of inositol 1,4,5-trisphosphate receptor types 1 and 3 in Ca^{2+} signaling, J. Biol. Chem. 279 (2004) 11967–11975.

[18] M. Iwai, T. Michikawa, I. Bosanac, M. Ikura, K. Mikoshiba, Molecular basis of the isoform-specific ligand binding affinity of inositol 1,4,5-trisphosphate receptors, J. Biol. Chem. (2007).